phys. stat. sol. (b) 89, 85 (1978)

Subject classification: 13.4; 22.1.2

Natuurkundig Laboratorium, Universiteit van Amsterdam[1])

Extended-Hückel-Theory Calculations for the Positive Divacancy in Silicon

By

C. A. J. AMMERLAAN and J. C. WOLFRAT

Calculations are carried out for the positive divacancy in silicon using the extended Hückel theory. These are non-iterative calculations in the molecular unit cell approach for various sizes of the unit cell and for various points in the Brillouin zone. The effects of two symmetry-allowed distortion modes of the six nearest-neighbour atoms of the divacancy are investigated. The parameters for stable Jahn-Teller distortion are determined by minimizing the extended-Hückel-theory energy. A second minimum with slightly higher energy is a saddle point with respect to distortions corresponding to other Jahn-Teller configurations. The energy barrier for reorientation between these configurations is obtained. From the wavefunction of the unpaired electron the hyperfine interaction with ^{29}Si nuclei in the two nearest-neighbour shells are calculated. For suitable distortions the results compare favourably with existing experimental data. A large discrepancy is found between the distortion parameters for minimum energy and for optimum match of the hyperfine constants.

Nicht-iterative Rechnungen werden für die positive Doppelleerstelle in Silizium mit Hilfe der erweiterten Hückel-Theorie ausgeführt. Es handelt sich hier um Rechnungen nach dem Verfahren der molekularen Einheitszelle für verschiedene Größe der Einheitszelle und für verschiedene Punkte in der Brillouin-Zone. Die sechs nächsten Nachbaratome der Doppelleerstelle werden systematisch in zwei von der Symmetrie erlaubten Verzerrungsmoden versetzt. Die Gleichgewichtslagen für Jahn-Teller-Relaxation werden bestimmt durch Minimalisierung der EHT-Energie. Ein zweites Minimum mit einer nur um wenig höheren Energie ist ein Sattelpunkt bezüglich der Verzerrungen, die mit den übrigen Jahn-Teller-Orientierungen zusammenhängen. Die Energiebarriere für Reorientierung zwischen unterschiedlichen Orientierungen wird ermittelt. Die Wellenfunktionskoeffizienten ermöglichen die Berechnung der Hyperfeinwechselwirkung zwischen dem ungepaarten Defektelektron und ^{29}Si-Kernen in den zwei Schalen der nächsten Nachbarn. Für geeignete Werte der Verzerrungsparameter existiert eine vernünftige Übereinstimmung mit zur Verfügung stehenden experimentellen Ergebnissen. Die Verzerrungskombinationen für minimale Energie und für das beste Resultat der Hyperfeinkonstanten weisen leider einen großen Unterschied auf.

1. Introduction

The extended Hückel theory is a semi-empirical, non-selfconsistent, one-electron approach [1]. The diagonal interaction matrix elements in the Hartree-Fock equations are approximated by experimental ionization energies and the non-diagonal ones by an empirical approximation, e.g. the Helmholtz-Wolfsberg assumption [2]. Though the method is lacking a justification from first principles it is frequently applied to calculate the electronic structure of deep level defects in covalent crystals [3, 4], like silicon [5, 6]. The advantages of the extended Hückel theory are its simplicity and its apparent ability to provide useful results for a number of properties. However, agreement between a few theoretical results and the corresponding experimental data may be fortuitous, or it may be attributed to a suitable adjustment of the free parameters in the semi-empirical theory. For a more detailed assessment of the merits of the extended Hückel theory calculations were carried out for a well-investigated defect in

[1]) Valckenierstraat 65, Amsterdam, Nederland.

a well-known solid: the divacancy, in its positive charge state, in silicon. The band structure of silicon is easily calculated using the extended Hückel theory [7]. Results can be made to compare satisfactorily with existing data [8, 9]. Many of the available experimental data for the divacancy in silicon, for example the electronic energy levels [8], the hyperfine interactions with ^{29}Si nuclei [10], and the response to stress, can also be obtained from the theory.

From observation of the electron paramagnetic resonance spectrum it was concluded that the lattice around the divacancy distorts [11]. This spontaneous distortion is a consequence of the Jahn-Teller instability of the partially filled doublet level. In the present work two symmetry-allowed distortions of the six nearest-neighbour atoms were considered as free parameters to optimize the calculated results. The extended-Hückel-theory energy, defined as the sum of the one-electron energies of the occupied levels [3], was determined and minimized to obtain the stable distortion. These calculations also yield the height of the energy barrier between different Jahn-Teller orientations [11]. From the wave function of the unpaired defect electron the hyperfine interactions with ^{29}Si nuclei on nearest-neighbour sites of the divacancy were calculated. These results are compared with the experimental data from measurements by electron paramagnetic resonance [11] and electron-nuclear double resonance [12].

2. Outline of Theory

2.1 Molecular orbitals

The one-electron eigenfunctions φ_i are expressed in Slater-type 3s and 3p atomic orbitals. These are given by $\chi_{3s} = N_s r^2 \exp(-\alpha_s r/a_0)$, $\chi_{3px} = N_p x r \exp(-\alpha_p r/a_0)$, etc., with the normalization constants $N_s^2 = (2\alpha_s/a_0)^7/2880\pi$, $N_p^2 = (2\alpha_p/a_0)^7/960\pi$, and Bohr radius $a_0 = 0.529 \times 10^{-10}$ m. For the orbital exponents the values $\alpha_s = 1.87$ and $\alpha_p = 1.60$ were used [13]. To reduce the required computer time symmetrized linear combinations of atomic orbitals were constructed. These symmetry orbitals σ_a are basis functions of the irreducible representations A_g, A_u, B_g, or B_u of the point group C_{2h} (2/m), which is the symmetry of the divacancy, consistent with the anisotropy observed in paramagnetic resonance spectra. The molecular orbitals φ_i are linear combinations of the symmetry orbitals, $\varphi_i = \sum_a c_{ai}\sigma_a$. The symmetry orbitals are associated with shells of symmetry-related atoms. There are two classes of shells. These are the general class shells containing four atoms each, and the mirror-plane class shells with only two atoms each related by inversion [12].

2.2 Molecular unit cell

An infinite solid is formed by periodic repetition of a unit cell [8, 14]. The corresponding wave functions are Bloch sums given by $\psi_{\boldsymbol{k},i}(\boldsymbol{r}) = N^{-1/2} \sum_{l=1}^{N} \exp(i\boldsymbol{k} \cdot \boldsymbol{R}_l) \times$ $\times \varphi_i(\boldsymbol{r} - \boldsymbol{R}_l)$, where the $\boldsymbol{R}_l$ represent the translation vectors of the lattice. Two atoms in the centre of the unit cell are removed to represent the divacancy. For a sufficiently large unit cell the interactions between defects in adjacent cells can be neglected. A unit cell consisting of 62 atoms plus divacancy is a cube with edge $2a$, when the edge of the usual non-primitive face-centred cubic unit cell is given length a. In the present calculations $a = 5.429 \times 10^{-10}$ m. The lattice is simple cubic with $2a\langle 100\rangle$ translation vectors. The C_{2h} symmetry of the unit cell is compatible only with a small number of wavevectors $\boldsymbol{k}$. Such vectors are $\boldsymbol{k} = \Gamma$, i.e. the centre of the Brillouin zone, and some of the X-, M-, and R-points on Brillouin zone boundaries. For a defect orientation having the $(01\bar{1})$ mirror plane these are $\boldsymbol{k} = X_1 = (\pi/a)$ [100], $M_1 = (\pi/a)$ [011], and $R_1 = (\pi/a)$ [111]. A unit cell of 52 atoms plus divacancy is

a regular rhombic dodecahedron. The associated translation vectors $\boldsymbol{R}_l$ are $(3a/2)\langle 011\rangle$. Calculations with C_{2h} symmetry are possible for $\boldsymbol{k} = \Gamma$, $X_1' = (2\pi/3a)$ [100], $R_1' = (\pi/3a)$ [111], and $R_2' = (\pi/3a)$ [$\bar{1}$11]. For a unit cell of 126 atoms plus divacancy the translational properties are similar to the 52 atom unit cell. This case requires a slightly modified set of shell orbitals to avoid coincidence of basis atoms on the boundaries of unit cells.

2.3 *Extended Hückel theory*

In the Hartree-Fock theory the eigenvalues E_i are the roots of the secular equation $\det |H_{ab\boldsymbol{k}} - E_i S_{ab\boldsymbol{k}}| = 0$. The wave function coefficients c_{ai} are obtained by solving the secular equations $\sum_a (H_{ab\boldsymbol{k}} - E_i S_{ab\boldsymbol{k}})\, c_{ai} = 0$. The interaction integrals $H_{ab\boldsymbol{k}}$ and overlap integrals $S_{ab\boldsymbol{k}}$ can be written as sums of integrals $H_{\mu\nu}$ and $S_{\mu\nu}$ involving atomic orbitals only [7]. For the overlap integrals $S_{\mu\nu} = \langle \chi_\mu \mid \chi_\nu \rangle$ of Slater-type atomic orbitals analytical expressions are available. The interaction integrals were reduced to these by applying the Helmholtz-Wolfsberg approximation [2]. These equate the diagonal elements $H_{\mu\mu}$ to the atomic ionization potentials I_{3s} or I_{3p}. The off-diagonal elements, $\mu \neq \nu$, are given by $H_{\mu\nu} = (1/2)\, K_{\mu\nu}(H_{\mu\mu} + H_{\nu\nu})\, S_{\mu\nu}$, with suitably chosen empirical constants $K_{\mu\nu}$. The present calculations were carried out with the values $I_{3s} = -14.95$ eV, $I_{3p} = -7.77$ eV, $K_{ss} = K_{pp} = 1.75$, and $K_{sp} = 1.313$ [13].

2.4 *Lattice distortions*

In the undistorted lattice the highest energy electron will occupy an orbitally degenerate level [11]. Due to the Jahn-Teller instability a spontaneous distortion will occur. Thereby the original D_{3d} symmetry is lowered to C_{2h}, which is the experimentally established symmetry of the divacancy [11]. The electronic degeneracy is removed. Considering only the six nearest neighbours of the divacancy there are 18 normal modes of distortion. Six of these reduce the symmetry to the required C_{2h} in one of the three orientations a distorted divacancy with given vacancy–vacancy axis can assume in the host lattice. For each of the three defect orientations only three normal modes are appropriate. One of these is a pure rotation. It was left out of consideration as for this mode the relative positions of the nearest-neighbour atoms do not change. Therefore, only two distortion modes remained for a systematic study of their effects. These modes, which were labelled EG1 and EG2, are illustrated in Fig. 1. Taking the origin of the coordinate system on the inversion centre of the divacancy, and using units of $a/8$, the nearest-neighbour-site positions are as given in Fig. 1. Atoms (133) and ($\bar{1}\bar{3}\bar{3}$) are on the mirror plane of the divacancy. The distortions are specified in Table 1. For one unit of distortion the r.m.s. displacement of the six nearest-neighbour atoms is equal to 1 Å.

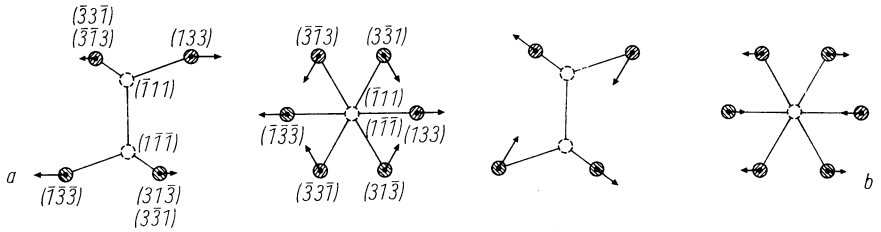

Fig. 1. The two symmetry-lowering distortion modes a) EG1 and b) EG2. Side view (left parts) and top view (right parts) of the divacancy (broken circles) and its six nearest neighbours (hatched circles). Arrows are drawn to scale corresponding to one unit of distortion

Table 1
Specification of the distortions EG1 and EG2

undistorted position	one unit of EG1 distortion	one unit of EG2 distortion
(133)	$(8\sqrt{6}/3a,\ 4\sqrt{6}/3a,\ 4\sqrt{6}/3a)$	$(8\sqrt{246}/123a,\ -56\sqrt{246}/123a,\ -56\sqrt{246}/123a)$
$(\bar{3}3\bar{1})$	$(-4\sqrt{6}/3a,\ -8\sqrt{6}/3a,\ 4\sqrt{6}/3a)$	$(-52\sqrt{246}/123a,\ 4\sqrt{246}/123a,\ 4\sqrt{246}/123a)$

The parameter a is a dimensionless quantity with the value of the lattice constant when expressed in Ångstroms. In the present calculations $a = 5.429$.

2.5 Hyperfine tensors

Once the wave function of the unpaired electron is known, the hyperfine interaction with the magnetic moments of ^{29}Si nuclei around the divacancy can be calculated. To avoid singularities in the hyperfine integrals the contact interaction arising from the non-zero value of the wave function at the nuclear site is dealt with separately. The major contribution to this isotropic interaction comes from the 3s orbital which has its centre on the hyperfine site. A probability density $|\psi_{3s}(0)|^2 = 31.5 \times \times 10^{24}$ cm^{-3}, calculated by Watkins and Corbett [15] on the basis of Watson and Freeman [16] atomic orbitals, rather than the vanishing value for Slater-type orbitals, was used. The dipole–dipole tensor components are given by $B_{\alpha\beta} = g_e\mu_B g_N\mu_N \times \times \langle\varphi_i|\,(3r_\alpha r_\beta - r^2\delta_{\alpha\beta})/r^5\,|\varphi_i\rangle$, with $\alpha, \beta = x, y,$ or z, and all other symbols having their usual meaning. The calculation requires the evaluation of various one-, two-, and three-centre integrals. Some explicit analytical expressions for these integrals are reported in a following paper [17]. For the quantity $\langle 1/r^3\rangle_{3p}$, appearing in the one-centre integrals, the value 16.1×10^{24} cm^{-3} was taken [15]. The calculated tensors were transformed to their principal axes systems. It was found convenient to equate the principal values in order of descending magnitude to $a + 2b$, $a - b + c$, and $a - b - - c$, respectively. Component a then describes the isotropic or contact interaction. The purely axial part is given by b, while c takes account of the deviations from axial symmetry.

3. Results

3.1 Energy levels

The one-electron energies E_i are the eigenvalues of the secular determinant. Fig. 2 shows these energy levels in a region near the bandgap calculated for the 62-atom unit cell for the points Γ, X_1, M_1, and R_1 in $\boldsymbol{k}$-space. For reference the energy positions for the top of the valence band at the Γ-point at $E_v = -7.75$ eV and for the bottom of the conduction band along the Δ-axis at $E_c = -6.67$ eV are also included. These values stem from an extended-Hückel-theory band structure calculation using the same parameters as for the present calculations for the solid with the defect. The levels labelled (1) are believed to originate from the divacancy. The corresponding states show a relatively high localization of the electron on the six nearest-neighbour atoms of the divacancy. Consequently, the sensitivity of these levels to distortion of the lattice near the defect is high and the $\boldsymbol{k}$-dependence is small. The levels are all located in the bandgap or in the valence band near the Γ-point band edge.

For a divacancy in the neutral charge state the 62-atom unit cell contains 248 electrons. Filling the levels from the bottom of the valence band upwards for the $\boldsymbol{k}$-points X_1, M_1, and R_1 this results in the three highest lying levels labelled (1) remaining empty.

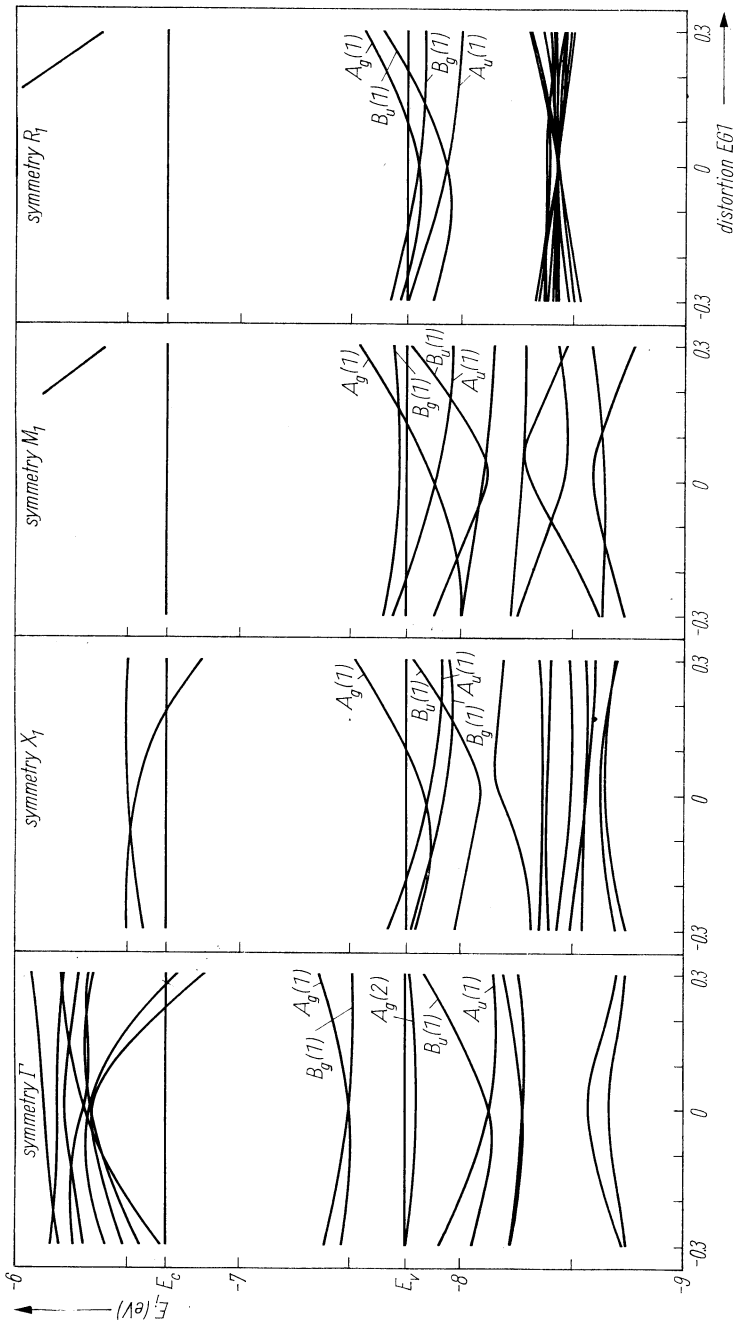

Fig. 2. Energies E_i of the one-electron states near the bandgap as function of the distortion parameter EG1 for the k-points a) Γ, b) X_1, c) M_1, and d) R_1; EG2 = 0. The valence and conduction band edges from the EHT band structure calculation are at E_v and E_c, respectively

The lowest of these four levels, always located 0.15 to 0.4 eV below the valence band edge E_v, is occupied by two electrons. From experiment it is known that the first donor level of the divacancy lies at 0.21 to 0.25 eV above E_v [11, 18]. Apparently, the extended Hückel theory predicts the divacancy-associated levels too low, possibly by about 0.5 eV. If one assumes this to be true for all $\boldsymbol{k}$-points, including the Γ-point, then in reality the levels $A_u(1)$ and $B_u(1)$ for the Γ-point are situated above the $A_g(2)$ level. The latter level should then be filled first. This procedure leaves two electrons for the (1)-levels, as is the case for the other $\boldsymbol{k}$-points. For the divacancy in the positive charge state one electron per unit cell is removed. The unpaired defect electron occupies the lowest of the four levels labelled (1). For nearly all distortions considered this level has A_u or B_u symmetry. An equivalent procedure to distribute the electrons over the eigenstates was followed for the 52- and 126-atom unit cells.

3.2 Total energy

The extended-Hückel-theory energy E_{EHT} of an electronic system is the sum of the one-electron energies E_i of the occupied levels. In the present case it is calculated by $E_{\mathrm{EHT}} = \sum_i n_i E_i$, with the occupation number $n_i = 2$ for $1 \leqq i \leqq 123$, $n_{124} = 1$, and $n_i = 0$ otherwise. For the 62-atom unit cell the extended-Hückel-theory energy was calculated systematically over the region $-0.3 \leqq \mathrm{EG1}, \mathrm{EG2} \leqq 0.3$, in steps of 0.1 for both the distortion parameters. This was done for the $\boldsymbol{k}$-points Γ, X_1, M_1, and R_1. The total energy E_{EHT} is a periodic function of the wavevector $\boldsymbol{k}$ in the reciprocal lattice. Using the method of Chadi and Cohen [19], the most accurate average of the energy over the Brillouin zone is given by $E^{\mathrm{AV}}_{\mathrm{EHT}} = [E_{\mathrm{EHT}}(\Gamma) + E_{\mathrm{EHT}}(X_1) + E_{\mathrm{EHT}}(M_1) + E_{\mathrm{EHT}}(R_1)]/4$. The resulting dependence of $E^{\mathrm{AV}}_{\mathrm{EHT}}$ on EG1 and EG2 is illustrated in Fig. 3. Similar results hold for each of the $\boldsymbol{k}$-points individually. Fig. 3 shows that two energy minima have developed, for almost opposite values of the distortion parameters. Near these minima the distortion dependence of the energy was examined more closely using a finer grid, with steps of 0.02, of the parameters. This way, the positions of the minima and the corresponding minimum values of E_{EHT} were determined more accurately. Also in these regions, calculations were performed exploiting only the S_2 symmetry of the divacancy. This allowed the calculations to be done for eight points in $\boldsymbol{k}$-space, i.e. Γ-point, all three X-points, all three M-points, and the R-point. A more reliable average over the Brillouin zone was thereby obtained [19]. The results are summarized in Table 2. Similar calculations near the energy minima were carried out for the 52-atom unit cell. Results are also presented in Table 2. Inspection of these data reveals that the values of the distortion parameters for the two minima do not depend very much on the $\boldsymbol{k}$-point chosen, or on the particular average over these points, nor on the size of the unit cell. It was therefore assumed that a similar behaviour of the energy will be shown for the 126-atom unit cell. The

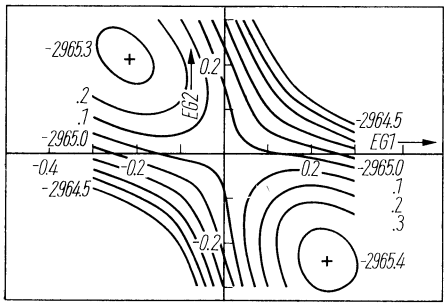

Fig. 3. Constant-energy contours of $E^{\mathrm{AV}}_{\mathrm{EHT}}$ calculated as an average over the Γ-, X_1-, M_1-, and R_1-points for the 62-atom unit cell. Distortions (EG1, EG2) for which the energy is a minimum are indicated by the symbol +

Table 2

Distortion parameters EG1 and EG2, and extended-Hückel-theory energies E_{EHT} for the two energy minima

size unit cell	k-point	EG1	EG2	E_{EHT} (eV)	EG1	EG2	E_{EHT} (eV)	E^{JT}_{EHT} (meV)
62	Γ	0.215	−0.229	−2963.756	−0.185	0.185	−2963.603	153
	X_1	0.242	−0.249	−2965.642	−0.242	0.212	−2965.726	− 84
	M_1	0.257	−0.258	−2966.966	−0.222	0.223	−2966.596	370
	R_1	0.231	−0.225	−2965.436	−0.224	0.223	−2965.380	56
	$(\Gamma + X_1 + M_1 + R_1)/4$	0.238	−0.241	−2965.447	−0.218	0.211	−2965.322	125
	$(\Gamma + 3X + 3M + R)/8$	0.236	−0.253	−2965.897	−0.227	0.213	−2965.756	141
52	Γ	0.194	−0.194	−2480.895	−0.171	0.163	−2480.833	62
	X_1	0.262	−0.217	−2486.938	−0.227	0.254	−2487.114	−176
	R_1	0.253	−0.279	−2485.453	−0.249	0.226	−2485.679	−226
	R_2	0.147	−0.158	−2486.373	−0.173	0.173	−2486.356	17
	$(\Gamma + X_1 + R_1 + R_2)/4$	0.230	−0.230	−2484.893	−0.209	0.207	−2484.980	− 87
	$(\Gamma + 3X + 4R)/8$	0.246	−0.249	−2485.634	−0.234	0.216	−2485.579	55
126	$(\Gamma + X_1 + R_1 + R_2)/4$	0.24	−0.25	−6038.233	−0.22	0.21	−6037.955	277

The (EG1, EG2) values for the 126-atom unit cell were not calculated, but were assumed, with reference to the smaller unit cells, to be close to the minima

time-consuming calculations for this large unit cell were restricted to the one particular choice of distortion parameters for each minimum as given in Table 2.

3.3 Reorientation barrier

The absolute minimum of the energy for (EG1, EG2) ≈ (0.24, −0.25) corresponds to the stable Jahn-Teller distortion of the divacancy. There exists a second minimum, with generally slightly higher energy, for a distortion ≈ (−0.22, 0.21). Thermally activated reorientation of the divacancy from an initial orientation to one of the other two Jahn-Teller distortions has been observed experimentally. In a transition from a given Jahn-Teller orientation to a second one, the symmetry of the defect halfway the transition is that of the third distortion. Moreover, the averaged distortion of the initial and final stable configurations is almost equal to the distortion in the relative minimum of the third configuration. It is likely therefore, that a transition between two stable distortions will occur via the relative minimum of the third orientation. The extended-Hückel-theory energy was calculated along a path of distortions from one configuration via a relative minimum to a second stable configuration. It was found that the relative minimum is a saddle point with respect to distortions corresponding

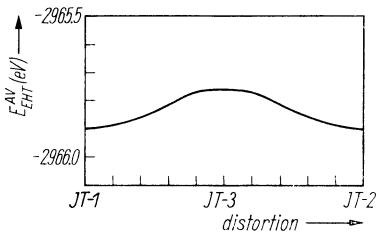

Fig. 4. The variation of the extended-Hückel-theory energy E^{AV}_{EHT} in a transition between the Jahn-Teller orientations 1 and 2 via the saddle point minimum of orientation JT-3

to other Jahn-Teller configurations. For intermediate distortions the energy varies monotonically between the stable absolute minimum and the saddle point maximum. Fig. 4 shows results from calculations using S_2 symmetry for the 62-atom unit cell for the average over eight $\boldsymbol{k}$-points in the Brillouin zone. The energy barrier for reorientation $E_{\mathrm{EHT}}^{\mathrm{JT}}$ is thus given by the difference of the energies for the relative and absolute minima. The values obtained for various $\boldsymbol{k}$-points and sizes of the unit cell are given in the last column of Table 2. These results have to be compared with the experimental value of 73 meV [11].

3.4 Hyperfine interactions

As mentioned in Section 2.5, and explained in detail in a following paper [17], the hyperfine tensor components can be calculated from the coefficients of the atomic orbitals. The present calculations were based on Γ-point orbitals of level $B_u(1)$ in a 62-atom unit cell. The required three-centre integrals for orbitals on nearest-neighbour positions of the hyperfine atom were computed numerically. As their contribution to the hyperfine tensors is small, in view of the approximations inherent in the theory, they were neglected. Results are reported only for the EG1 and EG2 distortions. Previous calculations have indicated that the breathing modes do not alter the results substantially, while also next-nearest-neighbour relaxations have a small effect [10]. Results for the mirror-plane shell, with the atoms (133) and $(\bar{1}\bar{3}\bar{3})$, are given in Fig. 5. The corresponding experimental results are $a = 148$ and $b = 28$ MHz [11]. For all distortions considered the theoretical value for the isotropic part of the hyperfine interaction is too low. However, by accepting a discrepancy between theory and experiment of 15% for both a and b, satisfactory match is obtained along a line extending from (EG1, EG2) $\approx$ (0.05, −0.05) to (0.3, 0.2). In the experiments no deviation from axial symmetry was reported. This is in agreement with the theoretical small value for c (133). For the nearest-neighbour general shell, consisting of the atoms on $(\bar{3}3\bar{1})$ and on the symmetry-related sites, the hyperfine results are presented in Fig. 6. The experimental hyperfine tensors labelled G1, with $a = 22.53$, $b = 1.94$, $c = 0.15$ MHz, and G2, with $a = 19.17$, $b = 0.63$, $c = 0.59$ MHz, are candidates for identification with this shell [12]. In the region (EG1, EG2) $\approx$ (0.1, 0.0) to (0.2, 0.1), which forms part of the region considered above, good agreement is obtained with the experimental tensor G1. Less satisfactory agreement exists for G2 as this tensor does not show the nearly axial symmetry required by the theory. In Fig. 5 and 6 the dis-

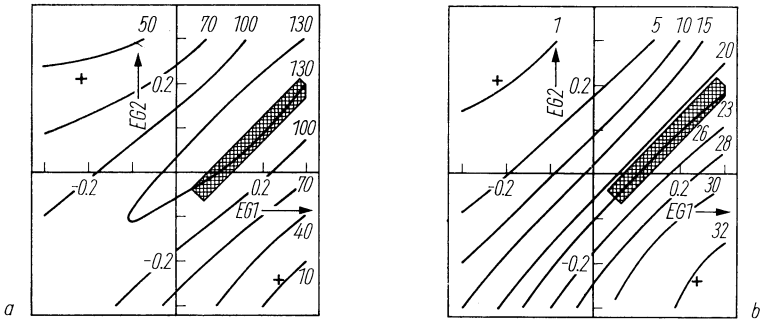

Fig. 5. a) Isotropic part a, b) axial part b (in MHz) of the hyperfine interaction tensor for shell (133) as function of the distortion parameters EG1 and EG2. The experimental values are $a \approx 148$, $b = 28$ MHz. A promising region of distortions is shown shaded. Distortions which minimize the energy are marked by +

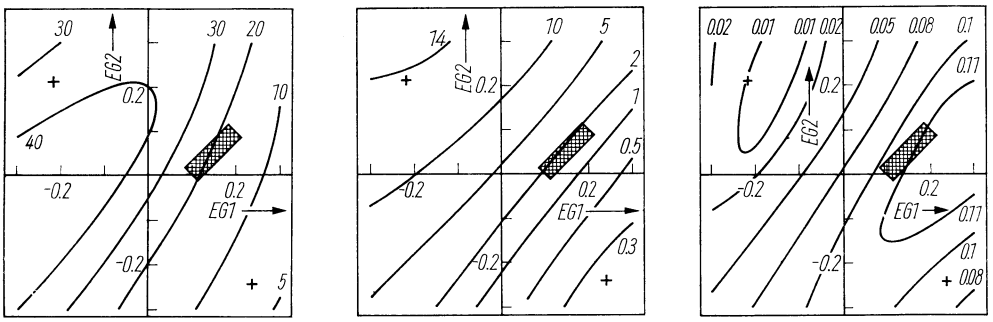

Fig. 6. a) Isotropic part a, b) axial part b, c) non-axial part c (in MHz) of the hyperfine interaction tensor for shell $(\bar{3}3\bar{1})$ as function of the distortion parameters EG1 and EG2. The experimental values are $a = 22.53$, $b = 1.94$, $c = 0.15$ MHz for tensor G1, and $a = 19.17$, $b = 0.63$, $c = 0.59$ MHz for tensor G2. A promising region of distortions is shown shaded. Distortions which minimize the energy are marked by +

tortion parameters (EG1, EG2) = (0.236, −0.253) and (−0.227, 0.213), which minimize the extended-Hückel-theory energy, are also indicated. For these distortions the calculated hyperfine tensor components show a poor resemblance with the experimental data.

4. Discussion

Obviously the most striking aspect of the results presented is the large discrepancy between the distortion parameters which minimize the total energy and those which give a best match of the hyperfine constants. This raises the question which of the properties is most reliably predicted by the theory: the energy or the wave function.

As far as energy is concerned, the highest energy level occupied for the neutral divacancy is found in the valence band. Certainly, for the highest donor state of the divacancy the level should have been in the bandgap. The stable distortion of the divacancy, obtained from minimizing the extended-Hückel-theory energy, is given by (EG1, EG2) $\approx$ (0.24, −0.25). For this set of distortion parameters, however, the level occupied by the unpaired electron has symmetry type A_u. This would imply an exactly vanishing contact interaction with ^{29}Si nuclei on the mirror plane of the divacancy, in contradiction with experimental findings. The positions of the energy minima, as shown in Table 2, have no strong sensitivity on the $\boldsymbol{k}$-value or on the size or shape of the unit cell. It is unlikely therefore that the particular choices of unit cell, or the way of averaging over the Brillouin zone, as in the present work, have affected the results substantially. For the Jahn-Teller barrier height only a correct order of magnitude is calculated. Surprisingly the smallest unit cell is best in this respect. The use of the extended-Hückel-theory energy as a measure of the total energy has been criticized strongly [20]. As electron–electron interactions are counted twice and nuclear–nuclear repulsion is omitted in the simple sum over one-electron energies this approximation to the total energy is probably grossly inaccurate.

Hyperfine tensor components for the two nearest-neighbour shells are predicted satisfactorily when the distortion is chosen for optimum match. The calculations were based on the wave function associated with level $B_u(1)$. At least for distortions (EG1 EG2) near (0.2, 0.1) this is the singly occupied level of which the unpaired electron is observed in EPR and ENDOR. The results for the general class shell, with atoms on $(\bar{3}3\bar{1})$ and on the symmetry-related sites, agree best with tensor G1. From the measure

ment of a motionally-averaged EPR spectrum it has been concluded, however, that tensor G2 is to be associated with the nearest-neighbour general class shell [11, 12]. The small difference between the averaged spectra, calculated by the choice of G1 or G2, leaves some doubt about this identification.

Both the energy considerations and the hyperfine interactions agree in their prediction of a positive value for EG1. This is consistent with results obtained from uniaxial stress experiments. For positive EG1 the bond length between the atoms $(\bar{3}3\bar{1})$ and $(\bar{3}\bar{1}3)$ and likewise that between $(31\bar{3})$ and $(3\bar{3}1)$ is reduced. The distance between the two atoms on the mirror plane increases. This is the kind of distortion expected for the Jahn-Teller effect. Inclusion of the distortion EG2 does not essentially alter this picture when the actual values found for EG2 are used. Therefore, a preference for the most probable sign of EG2 is not readily derived from these considerations.

Other sets of Slater orbital exponents have been suggested or used [5, 21]. Specific sets of parameters may lead to improved description of particular properties, e.g. the elastic constants, valence band states, or conduction bands. However, when a large number of data on different properties is involved a quantitative test of the extended Hückel theory is too severe a test. The present results therefore demonstrate the need for improvement of the theory of deep level defects in semiconductors.

References

[1] R. HOFFMANN, J. chem. Phys. **39**, 1397 (1963).
[2] L. HELMHOLTZ and M. WOLFSBERG, J. chem. Phys. **20**, 837 (1952).
[3] R. P. MESSMER and G. D. WATKINS, Phys. Rev. Letters **25**, 656 (1970).
[4] R. P. MESSMER and G. D. WATKINS, Phys. Rev. B **7**, 2568 (1973).
[5] KWOK LEUNG YIP, phys. stat. sol. (b) **66**, 619 (1974).
[6] VIJAG A. SINGH, C. WEIGEL, J. W. CORBETT, and L. M. ROTH, phys. stat. sol. (b) **81**, 637 (1977).
[7] R. P. MESSMER, Chem. Phys. Letters **11**, 589 (1971).
[8] T. F. LEE and T. C. MCGILL, J. Phys. C **6**, 3438 (1973).
[9] C. WEIGEL and C. A. J. AMMERLAAN, Verh. DPG (VI) **13**, 161 (1978).
[10] C. A. J. AMMERLAAN and C. WEIGEL, Radiation Effects in Semiconductors 1976, Ser. 31, Institute of Physics, London 1977 (p. 448).
[11] G. D. WATKINS and J. W. CORBETT, Phys. Rev. **138**, A543 (1965).
[12] J. G. DE WIT, E. G. SIEVERTS, and C. A. J. AMMERLAAN, Phys. Rev. B **14**, 3494 (1976).
[13] R. P. MESSMER, Lattice Defects in Semiconductors 1974, Ser. 23, Institute of Physics, London 1975 (p. 44).
[14] R. P. MESSMER and G. D. WATKINS, Radiation Damage and Defects in Semiconductors, Ser. 16, Institute of Physics, London 1973 (p. 255).
[15] G. D. WATKINS and J. W. CORBETT, Phys. Rev. **134**, A1359 (1964).
[16] R. E. WATSON and A. J. FREEMAN, Phys. Rev. **123**, 521 (1961).
[17] C. A. J. AMMERLAAN and J. C. WOLFRAT, phys. stat. sol. (b) **89**, No. 2 (1978).
[18] L. C. KIMERLING, see [10] (p. 221).
[19] D. J. CHADI and M. L. COHEN, Phys. Rev. B **8**, 5747 (1973).
[20] A. M. STONEHAM, Theory of Defects in Solids, Clarendon Press, Oxford 1975.
[21] E. CLEMENTI and D. L. RAIMONDI, J. chem. Phys. **38**, 2686 (1963).

(Received March 29, 1978)